Bull. Min. Res. Exp. (2018) 156: 137-150

Bulletin of the Mineral Research and Exploration

http://bulletin.mta.gov.tr

Mineralogical findings from manganese deposits in the Artova Ophiolite Complex, Derbent-Eymir area, Yozgat, Turkey

Nursel ÖKSÜZ[a*]

[a]*Bozok University, Engineering and Architecture Faculty, Department of Geological Engineering, Yozgat, Turkey. orcid.org/0000-0001-7371-3202*

Research Article

Keywords:
Artova ophiolite, manganese oxide, mineralogy, geochemistry, Yozgat-Turkey.

ABSTRACT

The Artova Ophiolitic Complex (AOC), which formed in association with Alpine Ophiolites, is exposed in the NE part of central Anatolia, in the interior of the central Black Sea region and within the borders of Çorum and Yozgat. The Derbent-Eymir manganese- oxide deposit under investigation occurs within this ophiolitic complex. The mineral association in Derbent ore is composed chiefly of pyrolusite, manganite and lesser amounts of ramsdellite, magnetite and goethite. Calcite is the main gangue mineral. The mineral association in Eymir ore is represented by pyrolusite, braunite, neltnerite, jacobsite, psilomelane and trace amount of limonite accompanied by some gangue minerals such as quartz and calcite. Electron microprobe analysis was carried out on pyrolusite, braunite and psilomelane minerals. While pyrolusite from Eymir has higher Si, Al, Mn and Ca, pyrolusite from the Derbent ore has lower Fe, K and Ba contents. Pyrolusite in the Eymir ore has higher Si, Al, Mn and Ca (10.28-7.06; 3.19-1.28; 87.98-81.88; 2.38-1.97 respectively) and lower Fe, K and Ba (0.31-0.16; 0.02-0.00; 0.07-0.00 respectively) contents in comparison to pyrolusite in the Derbent ore. Element variations in core-rim zones of spherical pyrolusites and manganite crystals elongated towards the gangue are quite noticeable. Both Eymir and Derbent ore deposits are low-temperature hydrothermal deposits. Geochemical variations recorded in various manganese minerals are found to be strongly dependent on the changes in pH and temperature of the ore-forming solution and distance to the spreading center.

Received Date: 21.02.2017
Accepted Date: 16.10.2017

1. Introduction

Turkey comprises an E-W trending component of the Alpine-Himalayan orogenic belt which occurs at the border between Laurasia to the north and Gondwana to the south. The Alpine-Himalayan orogenic system was formed by the closure of different branches of the Tethys Ocean. During the closure of the Tethys Ocean, various continental fragments of Laurasia and Gondwana collided. The land of Anatolia has been shaped as an orogenic collage which is composed of these continental fragments and the relict oceanic materials (radiolarian chert, basalt, pelagic shale, pelagic limestone, sandstone and serpentinite) between them (Okay and Tüysüz, 1999). The Artova Ophiolitic Complex (AOC) is one of the ophiolites tectonically sandwiched between the continental fragments and is a part of the Alpine-Himalayan orogenic system (Okay and Tüysüz, 1999). The manganese deposits in Derbent and Eymir (Yozgat) regions formed syngenetically associated with radiolarites in the Alpine ophiolite.

The present work focuses on the mineral paragenesis and geochemistry of manganese deposits in the Derbent and Eymir (Yozgat) areas. The manganese deposits are located 30 km NW and 80 km NE of Yozgat city, respectively. According to geological, mineralogical and geochemical data (major, trace and REE), the Derbent manganese deposit was formed by both hydrothermal and hydrogenous-diagenetic processes (Öksüz 2011*a*). The Eymir deposit was stated to be a volcanosedimentary type deposit where hydrothermal and hydrogenous processes exerted

* *Corresponding author: Nursel ÖKSÜZ, nursel.oksuz@bozok.edu.tr*
http://dx.doi.org/10.19111/bulletinofmre.334245

primary control (Öksüz, 2011*b*). Although Derbent and Eymir deposits are of the same type, their mineral associations are quite different. Thus, this work focuses on the examination of the geochemical and mineralogical variations in the Derbent and Eymir manganese deposits in order to infer which processes or factors were responsible for the observed differences. For this, the mineralogy of the ores was thoroughly examined (ore microscopy, X-ray diffraction, Raman spectroscopy and electron microprobe analysis) and ore paragenesis and structural-textural relations were determined.

2. Geological Setting

The lithologic units in the study area are composed of Paleozoic-Mesozoic metamorphics, radiolarite-bearing ophiolitic series, lower Eocene flysch, Lutetian transgressive series, Lutetian volcanic rocks and Neogene terrestrial sediments. The basement rocks are composed of metamorphic rocks of the Central Anatolian Massif consisting of quartzites, marbles, calcschists and amphibolite schists and crystalline rocks are represented by gabbro, diorite, granite and granodiorite. The basement rocks are overlain by the upper Cretaceous ophiolitic series rocks which are known as the Artova Ophiolitic Complex (AOC) (Özcan et al., 1980). The ophiolitic mélange is composed chiefly of limestone and marl, radiolarite, amygdaloidal basalt, pillow lava and serpentinites. Based on fossil assemblages recorded in the sedimentary units, the emplacement age of the ophiolite was dated to the Upper Cretaceous-Paleocene (Özcan et al., 1980). The lower Eocene sedimentary sequences in this region comprise turbidites which conform to the upper Cretaceous rocks. The basal conglomerate of the Lutetian unconformably overlies the lower Eocene units and partly the ophiolitic series. The lower Eocene units are characterized mostly by thick flysch layers, and lava and tuffs deposited in a shallow marine environment. The Lutetian volcanic series consists of lava including agglomerate, tuffs and tuffites of basaltic and andesitic composition. The upper Cretaceous and Lutetian units in the study area are the products of submarine volcanism (Özcan et al., 1980). The Neogene units consisting of sand, clay and lacustrine sediments are the youngest deposits in the region (Ketin, 1966; Akçay and Beyazpirinç, 2017; Figure 1). The ophiolitic series and lower Eocene rocks underwent several deformation events and therefore, metamorphics and crystalline basement rocks, serpentines and radiolarite-bearing ophiolitic series and lower Eocene layers were intensely fractured and folded.

The Derbent and Eymir manganese oxide deposits, located in the Çorum-Yozgat region in the NE part of central Anatolia and interior central Black Sea region, occur in the Artova Ophiolitic Complex (AOC) (Özcan et al., 1980), which formed in association

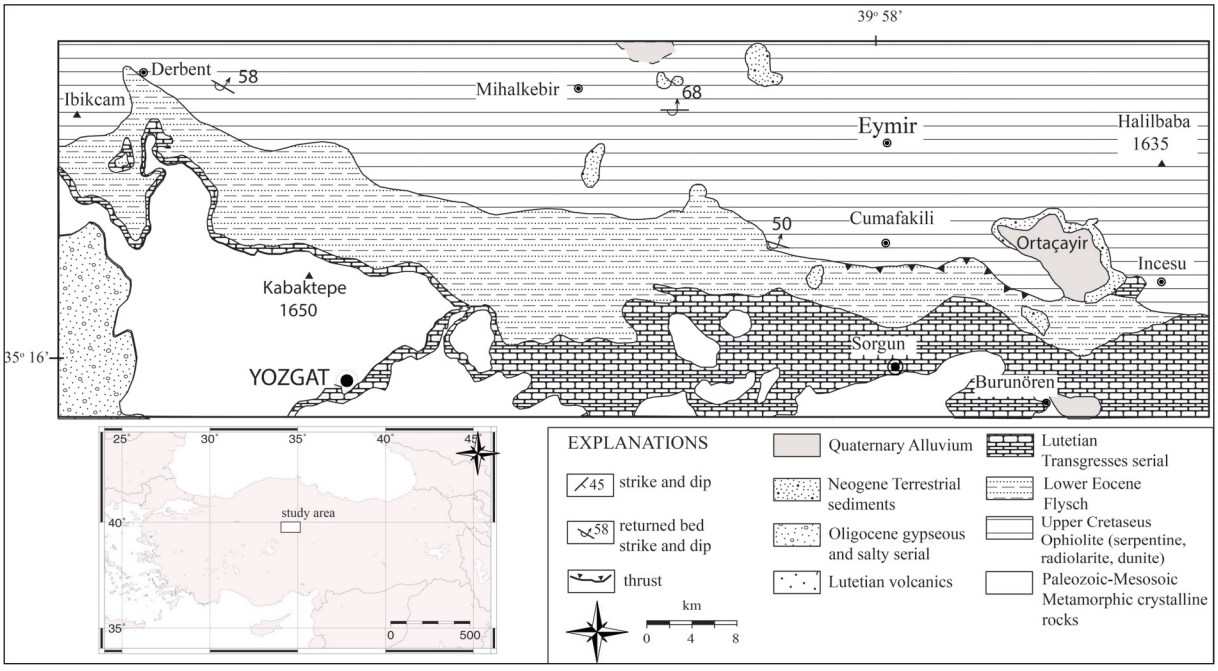

Figure 1- Location and geological map of the Derbent area (modified from Ketin 1966).

with Alpine ophiolites emplaced during the Turonian-Paleocene (Özcan et al., 1980). The manganese deposits in the study area are generally fractured and folded, developed in banded and lenticular shape, and are syngenetic with radiolarite cherts.

3. Materials and Methods

A total of 29 and 20 manganese ore samples (about 500 g) were collected from the Derbent and Eymir manganese oxide deposits, respectively. Forty-nine polished sections were studied with ore microscopy at the Bozok University Laboratory. Petrographic study was supported by X-ray diffraction analyses which were conducted on 10 samples at the of Turkish Petroleum Corporation (TPAO) Laboratories. X-Ray diffraction (XRD) analyses were carried out by a Philips PW 1800 diffractometer with a Cu anode operating at a generator voltage of 40 kV. Major oxide and trace element contents were determined using X-ray fluorescence (XRF) and inductively coupled plasma-optical emission spectrometry (ICP-OES), respectively, and REEs were analyzed via inductively coupled plasma-mass spectrometry (ICP-MS). Ore minerals were also studied with a Thermo Scientific DXR Raman Microscope at the Geological Department of Ankara University. The Raman spectra were evaluated with Crystal Sleuth program. Electron Probe Microanalyser (EPMA) analyses (backscattered electron (BSE) image) were performed by Cameca SX 100 at the laboratories of Austria Leoban University on a total of 51 points for selected pyrolusite, manganite, braunite and psilomelane. Microprobe analysis was conducted on spherical pyrolusite from core to rim of this mineral, while this analysis was done along a traverse from the ore mineral to the gangue (calcite) on elongated manganite.

4. Ore Geology

The deposit in the Derbent area is laminated (Figure 2A), but ore deposits in the Eymir area occur with laminated and lenticular shapes (Figure 2B). Both ore deposits are syngenetically hosted by the radiolarite cherts. The manganese ores associated with the radiolarites are intensively fractured and folded.

4.1. Ore Microscopy

The ore minerals in the Derbent area are mainly pyrolusite and manganite associated with trace amounts of ramsdellite, magnetite and goethite. In the Eymir area, the ore is composed of dominant pyrolusite, braunite, neltnerite, psilomelane and has trace amounts of limonite.

4.1.1. Manganese Minerals

Pyrolusite in Derbent has a typical spherical structure formed by the radiolarites. Radiolarian intervals are very common within the ore samples (Figure 3A). Pyrolusite veinlets occur due to the replacement of radiolarians. These are also present within the calcite veins (Figure 3B). Spherical pyrolusite crystals and radial pyrolusites with a core are observed (Figure 3B). Pyrolusites are mostly anhedral and subhedral. Spherical and radial pyrolusites surrounding a core and overlapping spherical crusts are also observed (Figure 3C, D).

Pyrolusite in this area is accompanied by magnetite and goethite (Figure 4A). The Raman spectra of pyrolusite are shown in figure 5A.

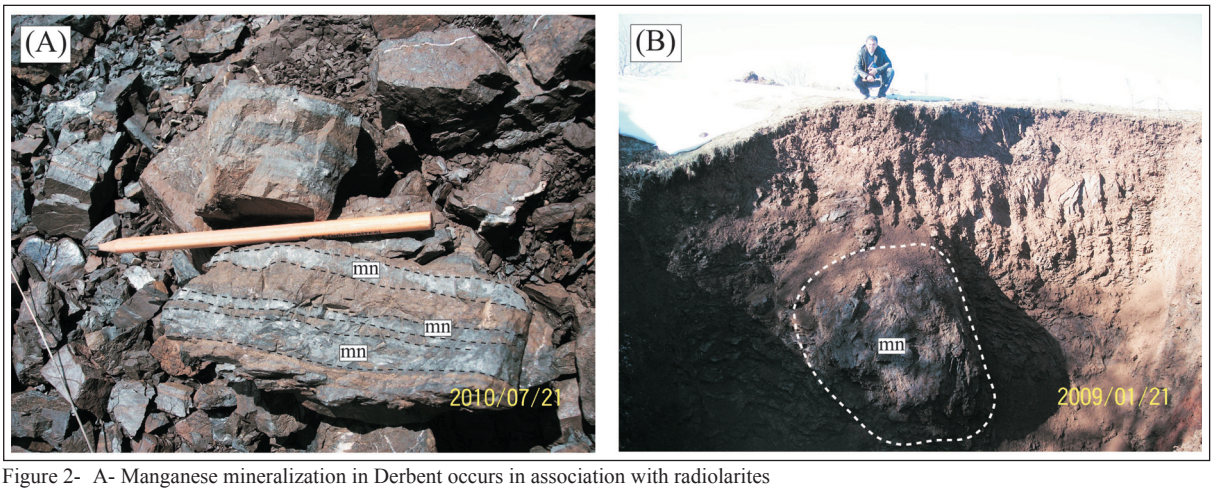

Figure 2- A- Manganese mineralization in Derbent occurs in association with radiolarites
B- Lens shaped mineralization in the Eymir deposit (rd: radiolarite, mn: manganese).

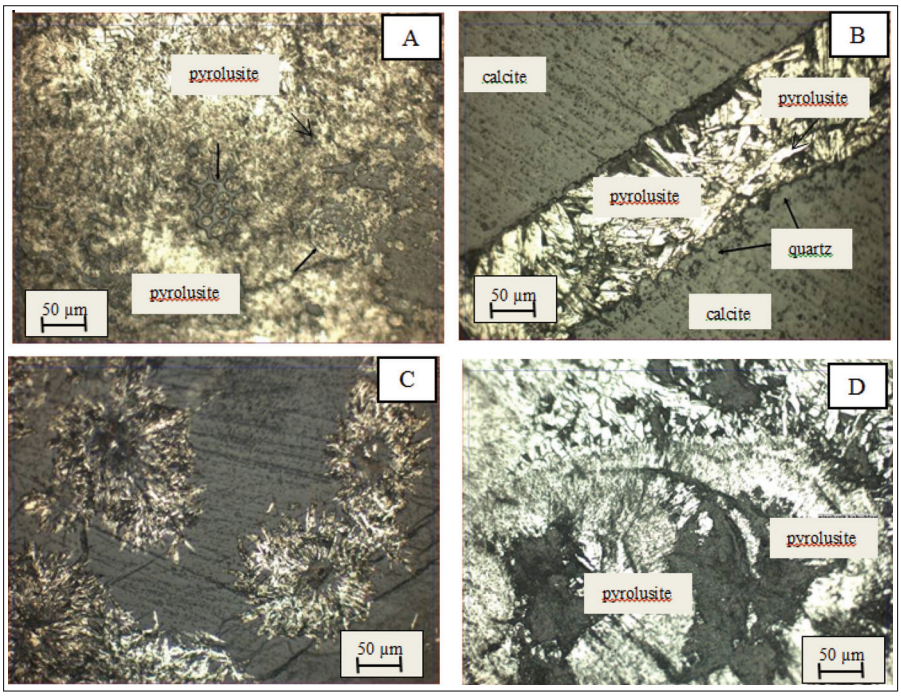

Figure 3- A- Different radiolarite remnants in Eymir: white and yellowish white parts ara pyrolusite, gray parts are gangue. Typical radiolarite remnants in Eymir (it show by arrow). 20x. B- Pyrolusite and quartz vein are settled in the cracks of calcite in Eymir. 20x. C- Radial pyrolusite occurring spherically around the core in Derbent. White and strong blue parts are gangue. 20x. D- The spherical pyrolusite substituted by the gangue in Eymir. Fibrous and barky pyrolusite in Derbent. 20x

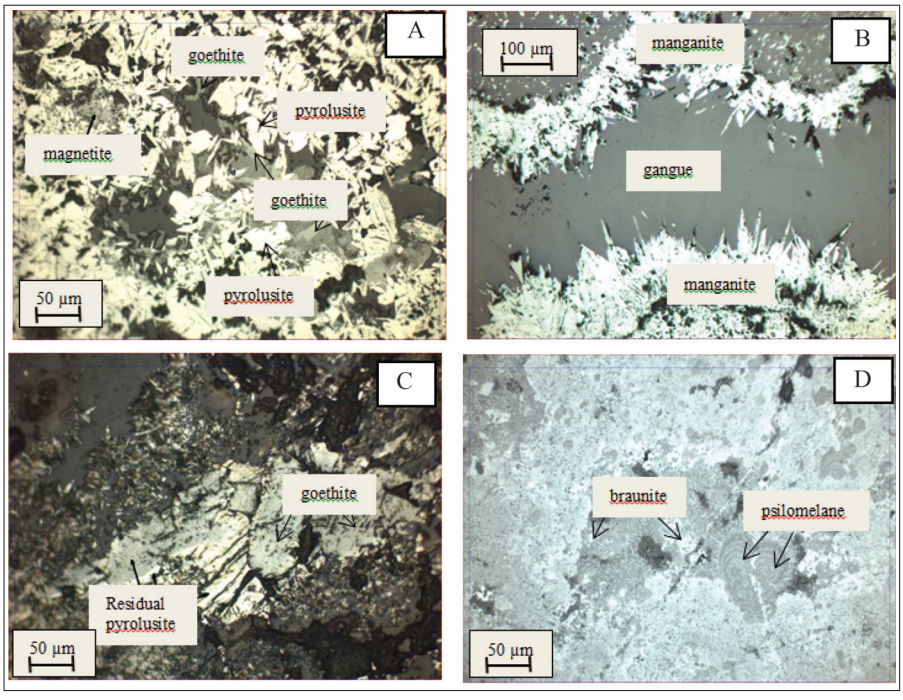

Figure 4- A- Magnetite, pyrolusite and pseudomorps of limonite and pyrolusite in Derbent. Dark gray and black are gangue (d: the pyrolusite is substituted the goethite from the edges of them) 20x. B- Manganite is shown as space filler in Derbent. Manganite crystals elongated towards the gangue (gangue is quartz) 10x. C- Goethiting of pyrolusite in Derbent mineralization. Whites are pyrolusite, grays are goethite. Pyrolusite remnants, thin vein and white parts are seen in goethite. 20x. D- Colloidal manganese mineralization consist of braunite and psilomelane in Eymir (white coloured minerals are braunite, gray coloured minerals are psilomelane). 20x.

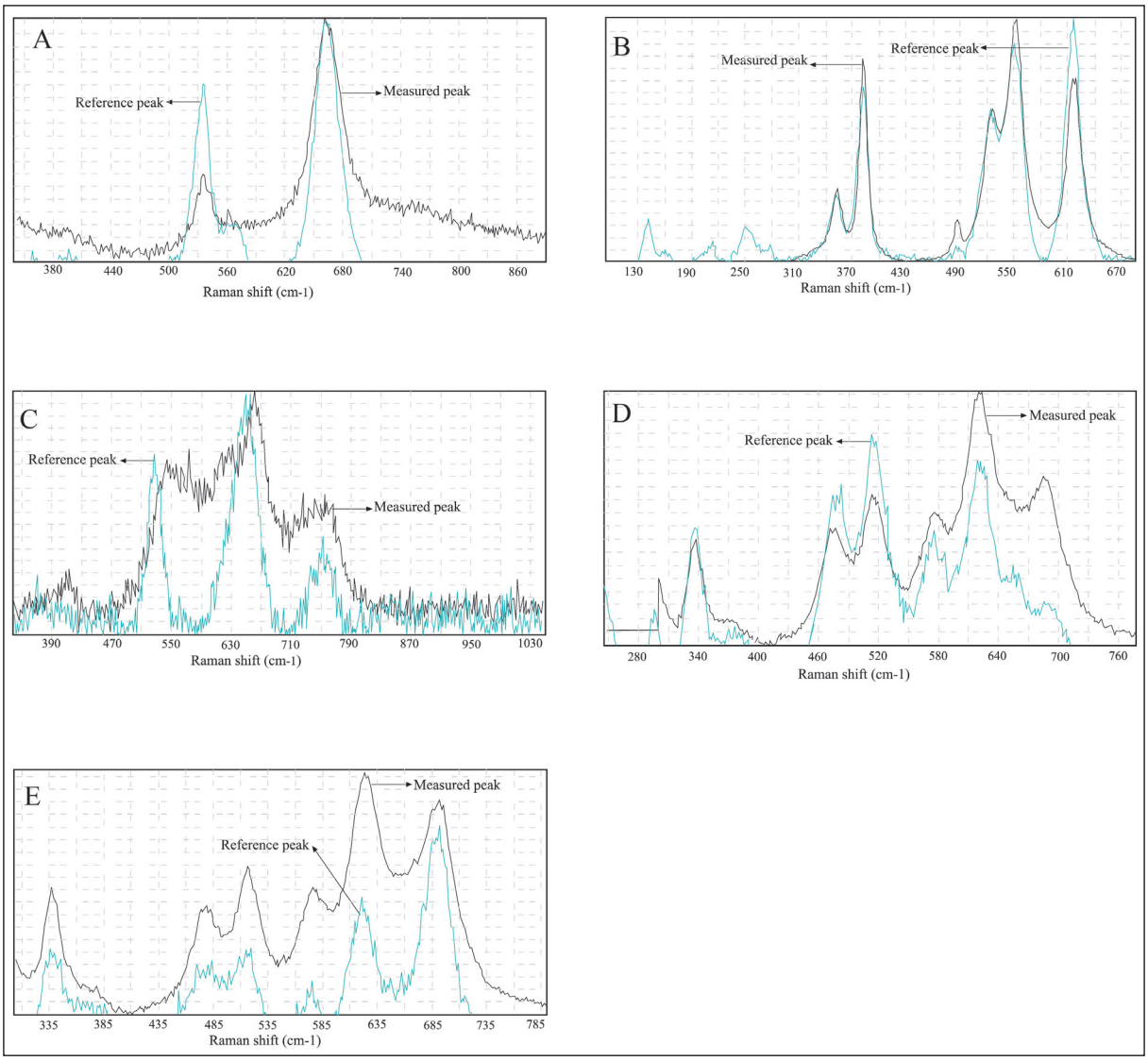

Figure 5- (A) Raman spectra of pyrolusite, (B) Raman spectra of manganite, (C) Raman spectra of ramsdellite, (D) Raman spectra of braunite, (E) Raman spectra of neltnerite.

Manganite is the main mineral in the Derbent deposit. The manganite is composed of radial crystals extending into the gangue (Figure 4B). It is also observed as interstitial fill and is noted for gray-brown color and strong anisotropy. Dissolution is also present in the form of capillaries in manganites. In addition, manganites are replaced by quartz. The Raman spectra of manganite are shown in figure 5B.

Ramsdellite was determined by the Raman spectra method (Figure 5C). A secondary mineral in manganese deposits, it formed by inversion of pyrolusite or oxidative dehydrogenation of groutite (Ramdohr, 1980).

Braunite and psilomelane are the most dominant minerals in the Eymir ore. Braunite is characteristic with slight brownish color and weak anisotropy. Psilomelane is gray color and displays strong anisotropy. In polished sections braunite and psilomelane are found together. Braunite associated with psilomelane in the deposit is characterized by colloidal textures and the psilomelane occurs as euhedral grains (Figure 4D). The Raman spectra of braunite are shown in figure 5D.

Neltnerite is the Ca-analogue of braunite observed in hydrothermal manganese oxide deposits (Baudracco-Grittie, 1985). Neltnerite is isostructural

with braunite. The Raman spectra of neltnerite are shown in figure 5E.

4.1.2. Iron Minerals

Magnetite and goethite in the Derbent ore are uncommon minerals and goethite mostly occurs due to alteration of pyrolusite (Figure 4C).

Jacobsite is observed to be associated with limonite as inclusions in pyrolusite. These pyrolusites are thought to be the product of inversion of jacobsite. The cracks within jacobsite are filled with gangue minerals. During this transformation, jacobsite becomes limonite with a greenish blue tone, replacing gray from the edges.

4.2. Mineral Chemistry

Microprobe analyses were conducted on pyrolusite, manganite, braunite and psilomelane from both Derbent and Eymir deposits. The analyses are shown in tables 1-3. Jacobsite and magnetite are too fine-grained to be analyzed.

Based on the results of microprobe analysis of pyrolusite samples, the average chemical formula of pyrolusite from the Derbent area was computed as $(Mn_{1.91\text{-}1.80}Fe_{0.03\text{-}0.01}Si_{0.03\text{-}0.01}Al_{0.07\text{-}0.01}K_{0.03\text{-}0.01}Ba_{0.03\text{-}0.00})O_2$ and from the Eymir area was computed as $(Mn_{1.59\text{-}1.36}Fe_{0.03\text{-}0.00}Si_{0.24\text{-}0.15}Al_{0.08\text{-}0.03}Ca_{0.05\text{-}0.04})O_2$.

Based on the results of microprobe analysis, pyrolusite from the Eymir ore (with average concentrations of Si: 9.81%; Al: 2.40%; Mn: 84.87%; Ca: 2.14%) has higher Si, Al and Ca content in comparison to pyrolusite from the Derbent ore (with average concentrations of Si: Si: 0.73%; Al: 1.64%; Mn: 94.16%; Ca: 0.28%). In addition, Fe, K and Ba concentrations in pyrolusite from the Eymir area (with average concentrations of Fe: 0.44%; K: 0.01%; Ba: 0.03%) are lower than those from the Derbent area (with average concentrations of Fe 0.85%; K 0.52%; Ba 1.20%) (Tables 1 to 3).

Mn, Fe, K and Ti concentrations from spherical pyrolusite crystals in the Derbent ore are found to increase from core to rim, while K content shows an inverse trend (Figure 6).

Based on the results of microprobe analysis of samples from the Derbent ore, the chemical formula of manganite was computed as $Mn_{1.97\text{-}1.91}Si_{0.04\text{-}0.01}O(OH)$ and the average composition is: Si = 0.91%; Fe = 0.11%; Al = 0.09%; Mn = 97.45%; Ca = 0.02%.

Mn, Si and Fe concentrations of elongated manganite crystals in the Derbent ore were examined and it was found that Mn and Si contents increase towards the gangue while Fe content first increases and then partly decreases (Figure 7).

Based on the results of microprobe analysis of samples from the Eymir ore, the chemical formulas of braunite and psilomelane were computed as, $(Mn_{10.29\text{-}9.18}Al_{0.27\text{-}0.05}Fe_{0.03\text{-}0.01}Ca_{0.51\text{-}0.31})O_8[Si_{1.09\text{-}0.60}O_4]$ and $(Si_{0.53\text{-}0.00}Al_{0.11\text{-}0.01}Ti_{0.08\text{-}0.00}Fe_{11.38\text{-}0.01}Mg_{0.49\text{-}0.00}Ca_{0.57\text{-}0.01})Mn_{13.61\text{-}0.00}O_{16}(OH)_4$ with average compositions of braunite and psilomelane of Si: 6.27%; Fe: 0.15%; Al: 0.94%; Mn: 89.21%; Ca: 2.66%, Si: 26.21%; Fe: 0.19%; Al: 0.33%; Mn: 69.97%; Ca: 2.29% respectively.

Table 1- Electron microprobe analyses of manganite (mn) and pyrolusite (pr) samples of Derbent manganese deposit

Samples elements	mn1	mn2	mn3	mn4	mn5	mn6	mn7	mn8	pr38	pr46	pr7	pr9	pr10	pr11	pr13	pr21	pr22	pr1
SiO_2	0.89	1.21	0.42	1.26	0.47	1.61	0.85	0.55	0.22	0.34	1.35	0.27	1.34	0.43	1.31	0.46	1.12	0.50
TiO_2	0.07	0.00	0.00	0.15	0.03	0.00	0.00	0.00	0.17	0.35	0.03	0.07	0.07	0.05	0.00	0.13	0.07	0.15
Al_2O_3	0.09	0.17	0.06	0.08	0.11	0.06	0.02	0.13	0.43	1.02	2.80	1.78	1.13	1.76	1.28	2.31	1.15	2.70
Fe_2O_3	0.16	0.14	0.17	0.16	0.09	0.06	0.09	0.04	1.00	1.70	0.37	0.93	0.76	0.81	0.69	0.44	0.77	1.04
MnO	97.30	96.53	98.21	96.94	98.20	96.96	97.24	98.21	94.03	94.06	94.02	95.33	95.99	95.68	92.41	92.49	93.25	94.35
MgO	0.18	0.13	0.17	0.22	0.15	0.27	0.18	0.27	0.07	0.10	0.08	0.05	0.12	0.08	0.00	0.03	0.05	0.15
CaO	0.03	0.03	0.01	0.00	0.04	0.00	0.01	0.01	0.35	0.41	0.22	0.27	0.22	0.20	0.31	0.22	0.34	0.22
Na_2O	0.00	0.00	0.00	0.00	0.11	0.00	0.00	0.00	0.22	0.05	0.00	0.00	0.00	0.00	0.08	0.08	0.11	0.00
K_2O	0.01	0.01	0.00	0.00	0.00	0.01	0.02	0.04	1.14	0.81	0.43	0.39	0.18	0.29	0.43	0.72	0.60	0.25
BaO	0.00	0.00	0.01	0.00	0.00	0.00	0.00	0.08	2.18	0.91	0.58	0.84	0.45	0.58	2.89	1.34	1.59	0.59
Total	98.73	98.22	99.05	98.81	99.20	98.97	98.41	99.33	99.81	99.75	99.88	99.93	100.26	99.88	99.40	98.22	99.05	99.95
Formulae on the basis of 2 Oxygenes																		
	mn1	mn2	mn3	mn4	mn5	mn6	mn7	mn8	pr38	pr46	pr7	pr9	pr10	pr11	pr13	pr21	pr22	pr1
Si	0.02	0.03	0.01	0.03	0.01	0.04	0.02	0.01	0.01	0.01	0.03	0.01	0.03	0.01	0.03	0.01	0.03	0.01
Ti	0.00	0.00	0.00	0.00	0.00	0.00	0.00	0.00	0.00	0.01	0.00	0.00	0.00	0.00	0.00	0.00	0.00	0.00
Al	0.00	0.00	0.00	0.00	0.00	0.00	0.00	0.00	0.01	0.03	0.07	0.05	0.03	0.05	0.04	0.06	0.03	0.07
Fe	0.00	0.00	0.00	0.00	0.00	0.00	0.00	0.00	0.02	0.03	0.01	0.02	0.01	0.02	0.01	0.01	0.02	0.02
Mn	1.94	1.93	1.97	1.92	1.96	1.91	1.95	1.96	1.91	1.87	1.80	1.88	1.86	1.88	1.85	1.85	1.86	1.83
Mg	0.01	0.00	0.01	0.01	0.01	0.01	0.01	0.01	0.00	0.00	0.00	0.00	0.00	0.00	0.00	0.00	0.00	0.01
Ca	0.00	0.00	0.00	0.00	0.00	0.00	0.00	0.00	0.01	0.01	0.01	0.01	0.01	0.00	0.01	0.01	0.01	0.01
Na	0.00	0.00	0.00	0.00	0.01	0.00	0.00	0.00	0.01	0.00	0.00	0.00	0.00	0.00	0.00	0.00	0.01	0.00
K	0.00	0.00	0.00	0.00	0.00	0.00	0.00	0.00	0.03	0.02	0.01	0.01	0.01	0.01	0.01	0.02	0.02	0.01
Ba	0.00	0.00	0.00	0.00	0.00	0.00	0.00	0.00	0.02	0.01	0.01	0.01	0.00	0.01	0.03	0.01	0.01	0.01
Total	1.98	1.97	1.99	1.97	1.99	1.96	1.98	1.99	2.03	1.99	1.94	1.98	1.96	1.97	1.99	1.98	1.98	1.96

Bull. Min. Res. Exp. (2018) 156: 137-150

Table 2- Electron microprobe analyses of braunite (br) samples of Eymir manganese deposit.

Samples element	br6	br8	br9	br12	br15	br16	br17	br19	br20	br21	br25
SiO_2	5.47	7.21	4.81	8.58	6.68	5.74	8.48	5.70	4.53	5.63	6.13
TiO_2	0.07	0.02	0.13	0.00	0.00	0.00	0.01	0.00	0.15	0.20	0.00
Al_2O_3	1.66	1.81	0.98	0.36	0.98	1.00	1.38	0.59	0.36	0.30	0.89
Fe_2O_3	0.29	0.16	0.06	0.16	0.07	0.10	0.23	0.07	0.19	0.16	0.16
MnO	88.01	87.33	91.04	87.23	89.32	90.06	86.03	90.58	91.72	90.33	89.71
MgO	0.22	0.15	0.12	0.08	0.02	0.13	0.15	0.05	0.00	0.00	0.12
CaO	3.71	2.24	2.31	2.70	2.55	2.49	2.38	2.87	2.62	2.64	2.70
Na_2O	0.00	0.00	0.11	0.00	0.00	0.05	0.00	0.00	0.00	0.00	0.00
K_2O	0.00	0.01	0.00	0.00	0.00	0.00	0.00	0.00	0.00	0.00	0.00
BaO	0.00	0.03	0.00	0.00	0.00	0.03	0.00	0.00	0.00	0.00	0.06
Total	99.43	98.96	99.56	99.11	99.62	99.60	98.66	99.86	99.57	99.26	99.77
Formulae on the basis of 12 Oxygenes											
	br6	**br8**	**br9**	**br12**	**br15**	**br16**	**br17**	**br19**	**br20**	**br21**	**br25**
Si	0.71	0.92	0.63	1.09	0.86	0.74	1.07	0.74	0.60	0.79	0.74
Ti	0.01	0.00	0.01	0.00	0.00	0.00	0.00	0.00	0.01	0.00	0.02
Al	0.25	0.27	0.15	0.05	0.15	0.15	0.20	0.09	0.06	0.14	0.05
Fe	0.03	0.02	0.01	0.02	0.01	0.01	0.02	0.01	0.02	0.02	0.02
Mn	9.61	9.40	10.12	9.35	9.70	9.89	9.18	9.97	10.29	9.80	10.03
Mg	0.04	0.03	0.02	0.02	0.00	0.03	0.03	0.01	0.00	0.02	0.00
Ca	0.51	0.31	0.32	0.37	0.35	0.35	0.32	0.40	0.37	0.37	0.37
Na	0.00	0.00	0.03	0.00	0.00	0.01	0.00	0.00	0.00	0.00	0.00
K	**0.00**	0.00	0.00	0.00	0.00	0.00	0.00	0.00	0.00	0.00	0.00
Ba	0.00	0.00	0.00	0.00	0.00	0.00	0.00	0.00	0.00	0.00	0.00
Total	11.16	10.95	11.29	10.89	11.07	11.19	10.83	11.21	11.36	11.14	11.22

Table 3- Electron microprobe analyses of psilomelane (ps) and pyrolusite (pr) samples of Eymir manganese deposit.

Samples element	ps10	ps11	ps12	ps14	ps15	ps16	ps17	ps19	ps21	ps22	ps35	pr1	pr2	pr3	pr4	pr6	pr7	pr8
SiO_2	25.78	28.88	33.89	21.53	14.38	22.83	32.35	30.02	26.04	22.13	30.53	7.06	8.79	9.17	12.32	9.36	11.72	10.28
TiO_2	0.08	0.03	0.05	0.00	0.00	0.03	0.00	0.00	0.20	0.00	0.05	0.00	0.03	0.03	0.00	0.00	0.03	0.03
Al_2O_3	0.51	0.17	0.25	0.38	0.21	0.19	0.57	0.25	0.36	0.26	0.43	1.28	3.14	2.12	3.06	2.59	1.44	3.19
Fe_2O_3	0.13	0.23	0.16	0.19	0.30	0.36	0.11	0.26	0.13	0.10	0.09	0.16	0.30	0.21	0.30	0.31	0.21	1.62
MnO	70.31	67.03	61.03	75.39	82.31	72.80	64.44	65.29	70.32	74.44	66.35	87.98	85.21	86.23	81.88	85.33	84.33	83.12
MgO	0.15	0.12	0.03	0.00	0.27	0.38	0.31	0.28	0.08	0.03	0.02	0.15	0.25	0.28	0.23	0.15	0.03	0.13
CaO	2.17	2.50	2.24	2.01	2.73	2.83	1.64	2.24	2.50	2.55	1.74	2.38	1.99	2.18	1.97	2.00	2.32	2.13
Na_2O	0.00	0.01	0.00	0.00	0.04	0.04	0.05	0.00	0.01	0.05	0.03	0.00	0.04	0.00	0.08	0.00	0.00	0.00
K_2O	0.02	0.00	0.02	0.00	0.00	0.05	0.04	0.00	0.01	0.01	0.01	0.02	0.00	0.00	0.00	0.00	0.00	0.02
BaO	0.03	0.07	0.07	0.00	0.17	0.17	0.30	0.11	0.04	0.09	0.07	0.03	0.04	0.04	0.00	0.00	0.00	0.07
Total	99.18	99.04	97.74	99.50	100.41	99.68	99.81	98.45	99.69	99.66	99.32	99.06	99.79	100.26	99.84	99.74	100.08	100.59
Formulae on the basis of 20 Oxygenes												**2 Oxygenes**						
	ps10	ps11	ps12	ps14	ps15	ps16	ps17	ps19	ps21	ps22	ps35	pr1	pr2	pr3	pr4	pr6	pr7	pr8
Si	4.49	4.90	5.53	3.92	2.81	4.09	5.27	5.05	4.51	0.00	0.01	0.15	0.18	0.19	0.24	0.19	0.23	0.20
Ti	0.01	0.00	0.01	0.00	0.00	0.00	0.00	0.00	0.03	0.06	0.08	0.00	0.00	0.00	0.00	0.00	0.00	0.00
Al	0.10	0.03	0.05	0.08	0.05	0.04	0.11	0.05	0.07	0.02	0.01	0.03	0.08	0.05	0.07	0.06	0.03	0.07
Fe	0.02	0.03	0.02	0.03	0.05	0.05	0.01	0.04	0.02	11.38	9.35	0.00	0.01	0.00	0.00	0.01	0.00	0.03
Mn	10.37	9.63	8.43	11.62	13.61	11.04	8.90	9.31	10.31	0.01	0.00	1.59	1.47	1.49	1.36	1.47	1.43	1.40
Mg	0.04	0.03	0.01	0.00	0.08	0.10	0.08	0.07	0.02	0.49	0.31	0.00	0.01	0.01	0.01	0.00	0.00	0.00
Ca	0.41	0.45	0.39	0.39	0.57	0.54	0.29	0.40	0.46	0.02	0.01	0.05	0.04	0.05	0.04	0.04	0.05	0.05
Na	0.00	0.00	0.00	0.00	0.02	0.01	0.02	0.00	0.00	0.00	0.00	0.00	0.00	0.00	0.00	0.00	0.00	0.00
K	0.00	0.00	0.00	0.00	0.00	0.01	0.01	0.00	0.00	0.01	0.01	0.00	0.00	0.00	0.00	0.00	0.00	0.00
Ba	0.00	0.00	0.00	0.00	0.01	0.01	0.02	0.01	0.00	0.00	0.00	0.00	0.00	0.00	0.00	0.00	0.00	0.00
Total	15.45	15.09	14.45	16.04	17.19	15.91	14.70	14.93	15.43	14.88	14.88	1.83	1.78	1.79	1.73	1.78	1.75	1.76

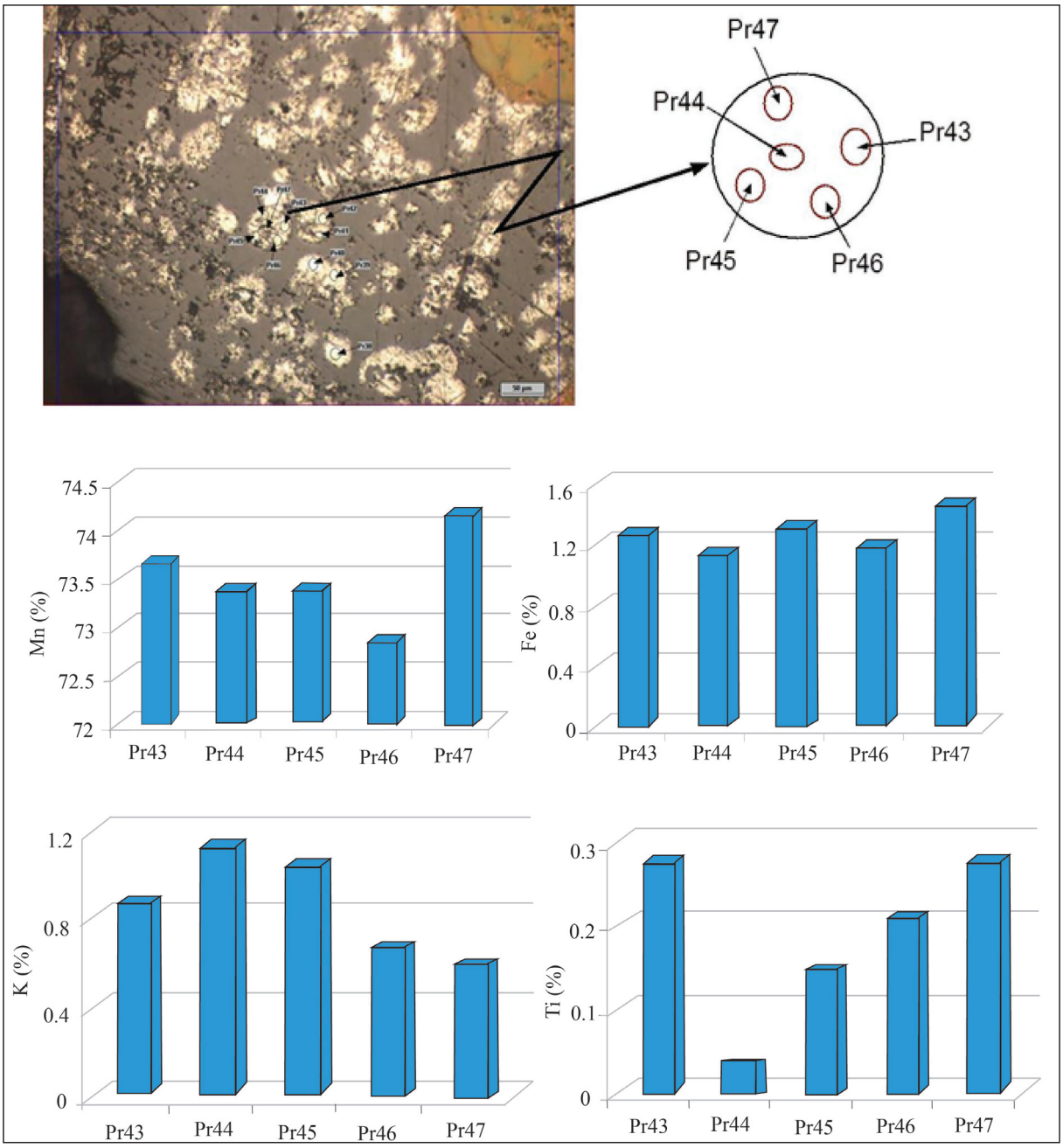

Figure 6- Signed microprobe points in spherical pyrolusite and variation diagram for Mn, Fe, Ti and K concentrations in Eymir region.

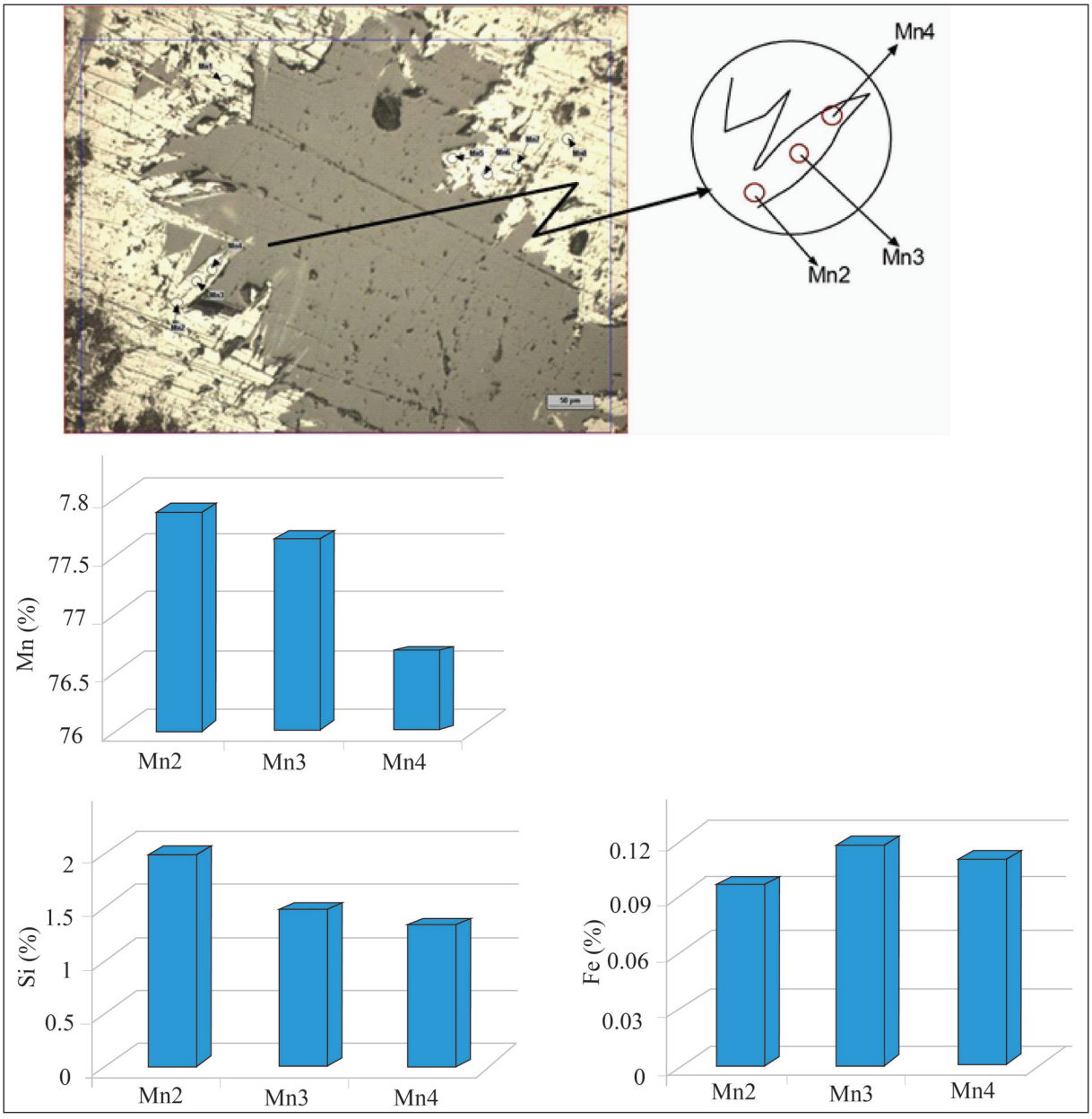

Figure 7- Microprobe measured points in manganite crystals and variation diagram for Mn, Si and Fe concentrations in Derbent region

5. Results and Discussion

The manganese deposits syngenetically occurred with radiolarites within the Artova Ophiolitic Complex (AOC) (Özcan et al., 1980) which developed within Turonian-Paleocene-aged Alpine ophiolitic series. The deposits were also affected by orogenic deformation in the region, thus they are intensely folded and fractured.

In the present work, manganese deposits in these areas were found to have similar geologic characteristics but ore paragenesis and ore mineral chemistry yielded different trends. According to some workers, certain manganese minerals reflect the properties of depositional environment and the origin of mineralization (Stanton, 1972; Roy, 1968; Nicholson, 1992*a,b*). For example, rhodochrosite, pyrolusite, cryptomelane, psilomelane and manganite are common manganese minerals within sedimentary deposits. Braunite generally occurs in volcanogenic deposits (Stanton, 1972). Jacobsite, spessartite and rhodonite are formed in metamorphic conditions

and are indicative of increasing temperature. Rhodochrosite occurs in sedimentary, hydrothermal and metamorphosed deposits and is deposited in moderately-reducing environments (Roy, 1968). Manganite, pyrolusite, psilomelane and cryptomelane are minerals characteristic of supergene conditions and are formed by the oxidation of primary manganese minerals (Ramdohr, 1980). Pyrolusite occurs in both supergene and hydrothermal environments and therefore is not an indicator of provenance (Nicholson, 1992*a, b*). It also forms in environments with high oxidation potential regardless of pH value (Krauskopf, 1989). Ramsdellite in the Derbent area is thought to be formed by transformation of pyrolusite. Pyrolusite and manganite are low-temperature minerals but braunite occurs at relatively higher temperatures (Roy, 1997).

Pyrolusite, which is mostly observed in low-temperature hydrothermal deposits, occurs due to the replacement of manganese oxide minerals like manganite and ramsdellite (Ramdohr, 1980). Pyrolusite is observed in both Derbent and Eymir ores. Pyrolusite in the Eymir area is thought to have a supergene origin (Öksüz, 2011*b*) as anhedral pyrolusite pseudomorphs are observed and Si, Al, Mn and Ca contents of pyrolusite in the Eymir ore are higher than those in the Derbent ore. Fe, K and Ba concentrations of pyrolusite in the Eymir area are lower than those in the Derbent area (Tables 1 and 3). Iron is the first soluble element and manganese stays in solution for a longer time (Nicholson, 1992*b*). Precipitation of iron and manganese from the solution requires gradual and regular change in the pH value (Hem, 1972; Krauskopf, 1989). Thus, Fe-rich minerals are found in areas close to the center of active submarine hydrothermal regions since their mobility is low, while manganese oxides are deposited in distal parts of the volcanic area (Choi and Hariya, 1992). Consequently, manganese oxide deposits (the presence of pyrolusite) are indicative of distal areas from spreading center. It is known that both deposits in the study area were rapidly deposited from hydrothermal solutions and are consistent with hydrothermal exhalative manganese deposits in modern spreading centers and formed in distal parts of spreading centers (Öksüz, 2011*b*). Moreover, data from this study indicates that pyrolusites in the Eymir area have higher Mn content and lower Fe content which might indicate that the deposit at Derbent is closer to the spreading center (Öksüz, 2011*a, b*; Öksüz and Okuyucu 2014).

Colloform texture is indicated by concentric rhythmic bands with concave-convex surface, in which the curvature is always convex towards the younger surface. Sometimes, it is observed as spheroid, mammillary, or botryoidal forms (Pettijohn, 1975; Salem, et al., 2012). Spherical and colloidal textures are created by precipitation from colloidal hot aqueous solutions or gels emerging from below (Salem et al., 2012). Space-fill texture is described as the deposition of younger minerals along vugs, fractures and cracks between the older ones. It is observed as the presence of quartz and calcite within manganese and iron minerals (Salem, et al., 2012).

Mn, Fe and Ti concentrations of spherical pyrolusite crystals in the Derbent ore are found to increase from core to rim while K content decreases from core to rim. Mn and Si concentrations of elongated manganite crystals at Derbent increase towards the gangue, while Fe content first increases and then partly decreases. This may be show the change in physicochemical conditions observed in the mineralization (Eh and / or Eh, T, P).

Results of paragenetic and geochemical evaluation indicate that deposits in the Eymir and Derbent areas are low-temperature hydrothermal deposits. Geochemical variations observed in the studied manganese minerals strongly depend on changes in pH-Eh and temperature of the ore-forming solution and distance to the spreading center.

Acknowledgements

This study is supported by The Scientific and Technological Research Council of Turkey (TUBITAK) (project no. 109Y167) and Bozok University Research Fund (project no. B.F.F.M/2009-06). The appreciation is extended to Dr. İbrahim Uysal for his help in EMP analysis.

References

Akçay, A.E., Beyazpirinç, M. 2017. The geologıcal evolution of Sorgun (Yozgat)-Yıldızeli (Sivas) foreland basin, petrographic, geochemical aspects and geochronology of the volcanism active in the basin Bull.Min.Res.Exp., 155, pp.71-80

Baudracco-Gritti, C. 1985. Subslilution du manganese bivalent par du calcium dans les mineraux du groupe: Braunite, neltnerite, braunite II. Bulletin de Mineralogie 108, 437-445.

Choi, J.H., Hariya, Y. 1992. Geochemistry and Depositional Environment of Mn Oxide deposits in the Tokoro Belt. Northeastern Hokkaido, Japan. Economic Geology, 87, 1265-1274.

Hem, J.D. 1972. Chemical Factors that Influence the Availability of Iron and Manganesein Agueous Systems. Geol. Soc. America Bull., 83, 443-450.

Ketin, İ. 1966. Tectonic Units of Anatolia. General Directorate of Mineral Research and Exploration Report no: 66, 20-34, Ankara (unpublished).

Krauskopf, K.B. 1989. Introduction to Geochemistry. McGraw-Hill International Editions, Earth and Planetary Science Series, Km Keong Printing Co. Pte. Ltd. Republic of Singapore 617.

Nicholson, K. 1992*a*. Genetic Types of Manganese Oxide Deposits in Scotland: Indicators of Paleo-Ocean-Spreading Rate and a Devonian Geochemical Mobility Boundary. Economic Geology 87, 1301-1309.

Nicholson, K. 1992*b*. Contrasting Mineralogical-Geochemical Signatures of Manganese Oxides: Guides to Metallogenesis. Economic Geology 87, 1253-1264.

Okay, A., Tüysüz, O. 1999. Tethyan Sutures of Northern Turkey. In: The Mediterranean Basins: Tertiary Extension Within the Alpine Orogen (eds. B. Durand, L. Jolivet, F. Horvath and M. Serrane), Geological Society of London, Special Publication, 156, 475-515.

Öksüz, N. 2011*a*. Geochemistry and the Origin of Manganese Mineralizations in Derbent (Turkey-Yozgat) Region. Bulletin of the Earth Sciences Application and Research Centre of Hacettepe University 32, 213-234

Öksüz, N. 2011*b*. Geochemical Characteristics of the Eymir (Sorgun-Yozgat) Manganese Deposit, Turkey. Journal of Rare Earths, 29 (3), 287-296.

Öksüz N., Okuyucu N. 2014. Mineralogy, Geochemistry, and Origin of Buyukmahal Manganese Mineralization in the Artova Ophiolitic Complex, Yozgat, Turkey. Journal of Chemistry Volume 2014, Article ID 837972, 11 pages http://dx.doi.org/10.1155/2014/837972

Özcan, A., Erkan, A., Keskin, E. 1980. General Geology of the North Anatolian Fault and Kirsehir Massif. General Directorate of Mineral Research and Exploration, Report no: 6722, Ankara (unpublished).

Pettijohn, F.G. 1975. Sedimentary rocks, 3rd edn. Harper and Row, New York, pp. 628.

Ramdohr, P. 1980. The Ore Minerals and Their Intergrowth. Pergamon Press, Oxford, London, New York.

Roy, S. 1968. Mineralogy of the Different Genetic Types of Manganese Deposits. Economic Geology, v. 63, pp. 760-786.

Roy, S. 1997. Genetic Diversity of Manganese Deposition in the Terrestrial Geological Record. In: Nicholson, K., Hein, J. R., Bühn, B. and Dasgupta, S. (eds). 1997. Manganese Mineralization: Geochemistry and Mineralogy of Terrestrial and Marine Deposits. Geological Society Special Publication, London, v. 119, pp. 5-27.

Salem, I.A., İbrahim, M. E., Monsef, M.A.E. 2012. Mineralogy, geochemistry, and origin of hydrothermal manganese veins at Wadi Malik, Southern Eastern Desert, Egypt Arabian Journal of Geosciences, v. 5, pp. 385-406.

Stanton, R.L. 1972. Ore Petrology. McGraw-Hill, New York.